Investigation on stress-induced effect of luminescence properties of blue/violet LEDs

CHE YUANG, WANG DANGHUI*, ZHANG LINGKUN, YUAN TIANHAO, ZHANG MENGFAN, ZHANG SHUYAN, GUO YUYANG, WU YUHAO, CAO XIYUE

College of New Energy of Xi'an Shiyou University, Xi'an 710065, China

Nowadays, III-nitride MQW blue/violet light-emitting diodes (LEDs) exhibit exemplary characteristics in a multitude of applications, including high-brightness illumination, white light generation, full-color display, water purification, and ultraviolet identification technology. In this study, the residual stress/strain existed in the active region of the bandgap, luminescence properties, and electrical properties of violet (AlGaN/GaN) and blue (InGaN/GaN) light-emitting diodes (LEDs) using the APSYS software. The findings suggest that there is a sensitive stress-dependent relationship between the bandgap, carrier concentration, optical output power and threshold voltage and stress/strain. As stress/strain increases, blue/violet LED devices exhibit band tilt, a reduction in carrier concentration, optical output power attenuation, an expansion of the band gap width and an elevation in threshold voltage. In comparison to the blue LED, the violet LED is more susceptible to the effects of stress on its luminous properties. The findings offer a foundation for further investigation into the optimisation and enhancement of the luminous and electrical properties of short-wave LEDs through the modulation of stress.

(Received March 6, 2024; accepted October 7, 2024)

Keywords: Blue/violet LED, Multiple quantum wells, Stress, Optoelectronic properties

1. Introduction

Gallium nitride (GaN)-based light-emitting diodes (LEDs) have become a prevalent technology in a number of fields, including high-quality lighting, full-color display, biology, and medical applications. This is largely due to the superior luminous efficiency, extended lifetime, and reduced power consumption that GaN-based LEDs offer compared to traditional technologies. [1-3] Residual stress/strain in the active region, resulting from parameter and thermal-expansion coefficient mismatches between the substrate and epitaxial films, has emerged as a significant factor influencing the luminous efficiency, quality, and reliability of short-wavelength LEDs. [4-6]. The majority of researchers have employed various techniques to mitigate or eliminate stress and strain, with the objective of enhancing the quantum efficiency of polarity LEDs. These techniques encompass superlattice, composition-graded, and size-graded MQWs, among others. As well known, the stress field and polarization effect are complex synergistic system for wurtzite lattice structure [7]. The reduction or elimination of the influence of stress/strain on the luminous properties of short-wavelength LEDs has become a pivotal concern in the commercialization of blue/violet LEDs.

The stress field in the GaN-based blue/violet LED MQW is relatively complex due to the thin thickness of the potential well layer and barrier layer. The polarization effect (including spontaneous polarization and piezoelectric polarization) of AlGaN and InGaN ternary compounds induces a built-in electric field in the active region, tilts the band gaps and reduces the luminescence and electrical properties of blue/violet LEDs. When piezoelectric polarization is caused by the stress field, it usually causes a change in the built-in field, which tilts the bandgap in the active region at the interface between InGaN and AlGaN, affects the radiative recombination, leads to a redshift in the luminous wavelength and reduces the luminous efficiency of the LED [8].

In order to eliminate the influence of the stress field, researchers have achieved some results by employing techniques such as the utilisation of a GaN buffer layer, an AlN nucleation layer, and an AlGaN/GaN superlattice layer. These methods have been shown to not only yield high-quality epitaxial films, but also to enhance the stress conditions within these films. [9,10]. Furthermore, the stress in the active region of LEDs can be managed through techniques such as composition-graded [11], thickness-graded MQWs [12], and growth along non-polar or semi-polar directions, which can effectively mitigate the impact of stress-induced effects in the active region [13].

According to the principle of Raman spectroscopy, the relationships between the residual stress and the Raman shift in the epitaxial film of GaN-based LED are elucidated by the following Eq. (1):

$$\Delta\sigma = \frac{\Delta\omega}{k} \tag{1}$$

where $\Delta\sigma$ is the in-plane stress, $\Delta\omega$ is the Raman shift, and k is the linear stress-shift coefficient of the biaxial stress system (k=2.40 cm^{-1}/GPa). In Ref. [14] the residual stress in GaN epitaxial films can be evaluated between 1.04 GPa

and 1.53 GPa. In this study, we employed APSYS software and set up the stress range from 0.0 GPa up to 2.0 GPa, and modeled AlGaN/GaN MQW violet LED and InGaN/GaN MQW blue LED, respectively, and analyzed the influence of stress-induced on the luminous properties and electrical properties of MQW LEDs.

2. Modeling

A schematic diagram of the structures of blue/violet LEDs is shown in Fig. 1. The size of LEDs is 350 μm × 350 μm, and the growth direction is [0001]. The violet LED comprises a sapphire substrate with a thickness of 430 μm, an n-AlGaN layer with a thickness of 4 μm and a doping concentration of 5×10^{18} cm^{-3}, five pairs of $Al_{0.056}Ga_{0.944}N$/GaN (10 nm/6 nm) quantum wells, an electron-blocking layer (EBL) was formed by a p-$Al_{0.15}Ga_{0.85}N$ layer with a thickness of 20 nm, an AlGaN layer with a thickness of 0.1 μm and doping concentration of 2×10^{19} cm^{-3} and a p-GaN layer with a thickness of 0.2 μm and a doping concentration of 1×10^{20} cm^{-3}. For the blue LED, consisting of a sapphire substrate with a thickness of 430 μm, an n-InGaN layer with a thickness of 4 μm and a doping concentration of 5×10^{18} cm^{-3}, five pairs of $In_{0.1}Ga_{0.9}N$/GaN (6 nm/10 nm) quantum wells, an EBL formed by a 20 nm thicknessed p-$In_{0.2}Ga_{0.8}N$ layer, a 0.1 μm thicknessed and 2×10^{19} cm^{-3} doped InGaN layer, and a 0.2 μm thicknessed and 1×10^{20} cm^{-3} doped p-GaN. The device size is consistent with the growth direction and violet LED.

3. Analysis of the optical properties of LEDs

3.1. Bandgap diagram

Fig. 2 illustrates the MQW bandgap diagram of violet and blue LEDs subjected to the specific stress conditions under investigation. As can be seen from Fig. 2(a), for the violet LED, the application of stress causes a tilting of the conduction and valence bands for the violet LED. However, the effect on the valence band is significantly less

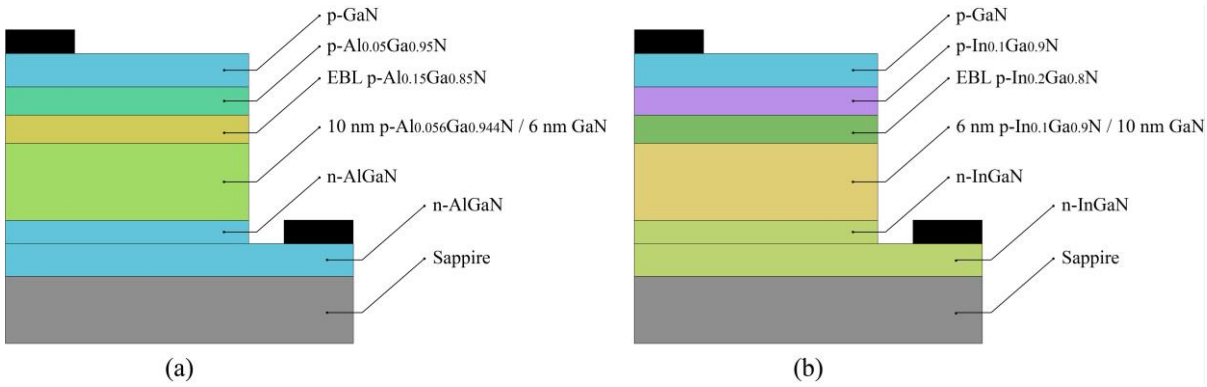

Fig. 1. Schematic diagram of the studied LEDs: (a) Violet LED; (b) Blue LED (color online)

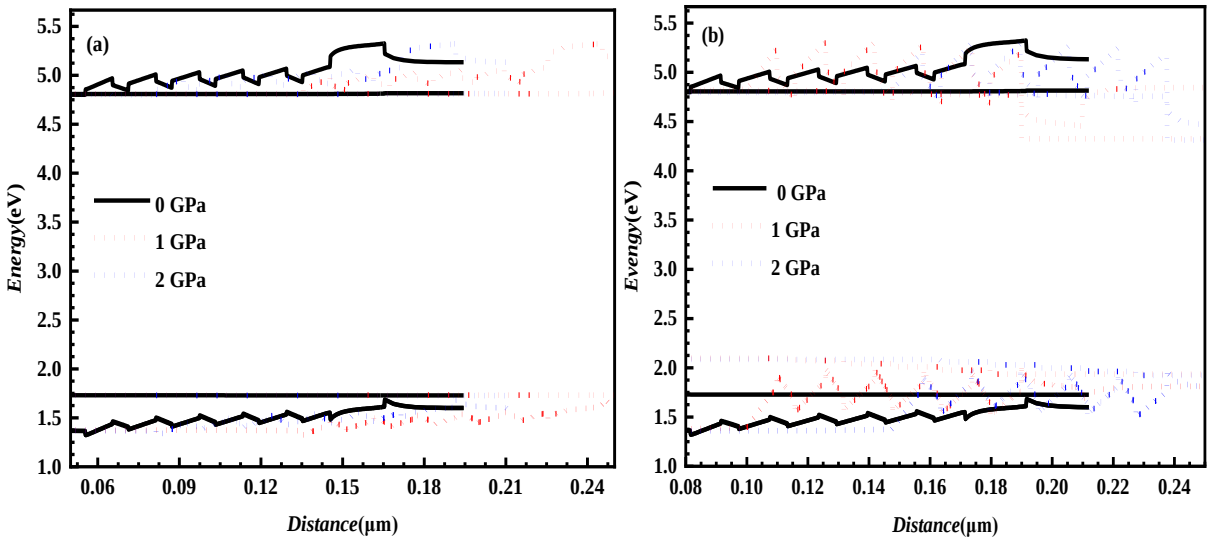

Fig. 2. Bandgap diagram of the MQW LEDs under the studied stress: (a) Violet LED; (b) Blue LED (color online)

pronounced than that observed for the conduction band. This is particularly evident in the effective barrier observed in the conduction band, which can be attributed to the piezoelectric polarization field of the potential well and the barrier layer in the quantum well. This phenomenon leads to the separation of electrons and holes in the bandgap, reducing electron leakage and consequently enhancing the radiative recombination probability and luminous efficiency of the LED. The impact of stress on the blue LED, as illustrated in Fig. 2(b), is more pronounced in both the conduction band and the valence band. This is evident from the tilt of the bandgap diagram of MQWs. In addition, one can observe from Fig. 2(a) and Fig. 2(b), the effect of the stress field on the last barrier and the EBL in MQWs is more evident due to the introduction of a polarized electric field at the interface [15,16].

3.2. Carrier concentrations

The distributions of electron and hole concentrations in the violet LED and the blue LED, as a function of the applied stresses, are illustrated in Fig. 3 and Fig. 4, respectively. As can be seen in Fig. 3, for the violet LED, the higher concentration of electrons in the first and last quantum wells is due to the injection of electrons into the light-emitting active region from the n-type region, the first quantum well is close to the n-type region resulting in a higher concentration of electrons, and the last quantum well is close to the p-type region, and more electrons are confined to the last quantum well due to the existence of the electron barrier layer restricting the escape of electrons. The

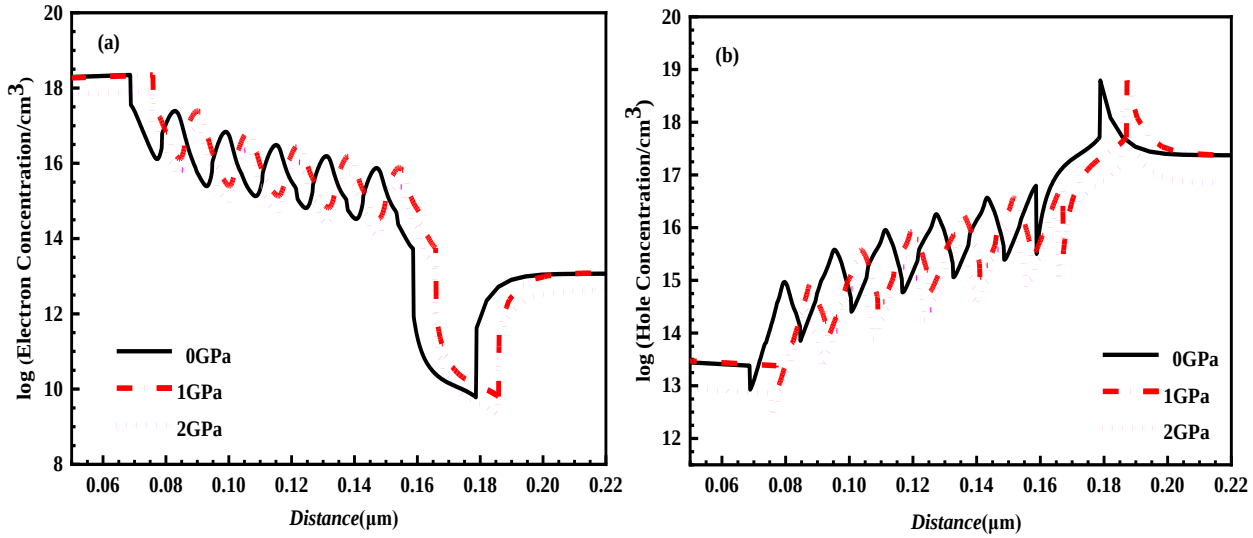

Fig. 3. Electron-hole concentration distribution of violet LED under the studied stress: (a) Electron concentration; (b) Hole concentration (color online)

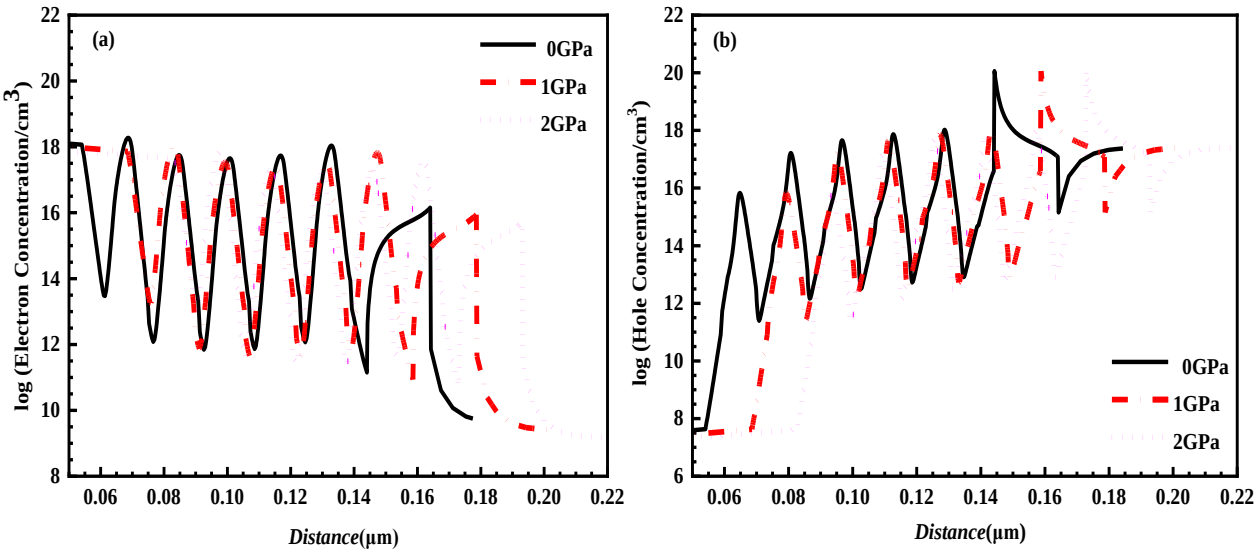

Fig. 4. Electron-hole concentration distribution of blue LED under the studied stress: (a) Electron concentration; (b) Hole concentration (color online)

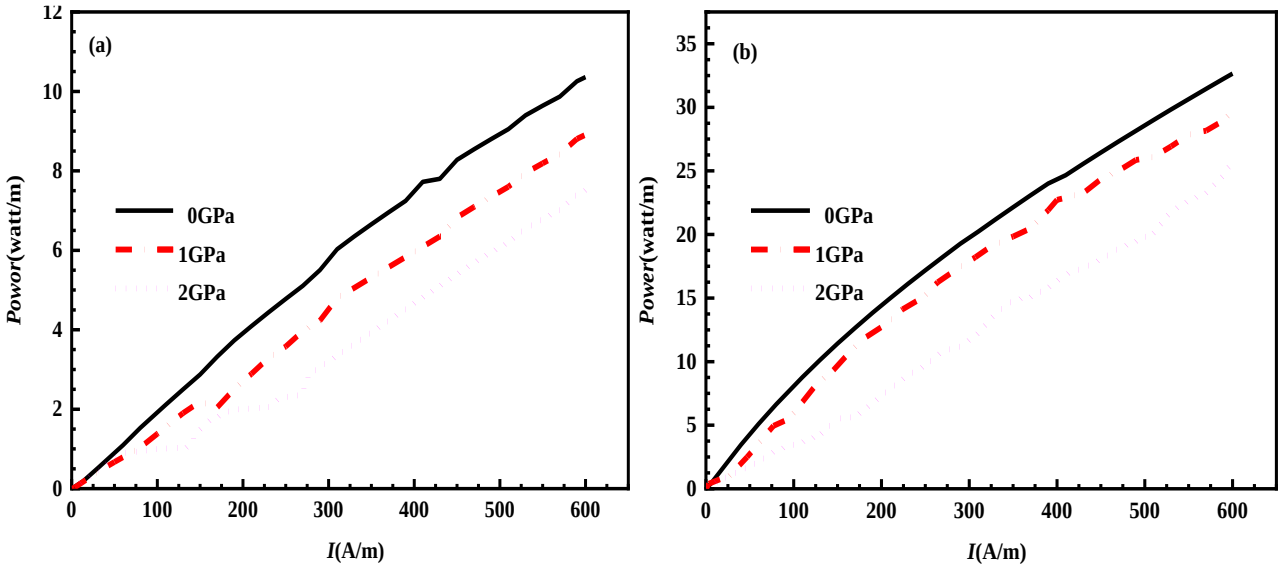

Fig. 5. Optical output power diagram of LEDs under the studied stress: (a) Violet LED; (b) Blue LED (color online)

distribution of holes in the quantum well is relatively uniform. In comparison to 0 GPa, the concentration of electrons and holes exhibits a slight decrease at 1 GPa and 2 GPa stresses, which consequently leads to a reduction in the luminous efficiency of violet LEDs with increasing stress. From Fig. 4, for the blue LED, the average hole concentration in quantum wells is much smaller than that of electrons. In comparison to holes, electrons possess a smaller effective mass and higher mobility. Consequently, electrons are more readily injected from the n-type region to the p-type region under the influence of the polarized electric field, resulting in electron leakage. Conversely, holes, with their greater effective mass and lower mobility, exhibit a generally lower injection efficiency in LEDs, which affects the luminous efficiency of blue LEDs.

3.3. Optical output power

Fig. 5 shows the correlation between light output power and current density for violet and blue LEDs subjected to the different stresses. As illustrated in Fig. 5, the light output power of both LED devices exhibited a decline in response to an increase in stress at a constant current density injection. At the maximum current density of 600 A/m, an increase in stress from 0 GPa to 2 GPa was observed to result in a decrease in light output power for both the violet LED (27.90%) and the blue LED (21.67%). A comparative analysis reveals that the impact of stress on the light output power of the violet LED is more pronounced than that of the blue LED.

3.4. Effect of stress on the bandgap

The bandgap of III-nitride compound materials varies with the stress can be expressed by Eq. (2) [17]:

$$E_g(P) = E_g(0) + \alpha P + \beta P^2 \tag{2}$$

where $E_g(0)$ is the bandgap of the stress-free material, P is the stress, α and β are the pressure parameters. α and β values for the InN, GaN, and AlN materials are shown in Tab. 1.

Table 1. Stress-induced coefficients in III-nitride materials [18-20]

Parameter	Unit	AlN	GaN	InN
α	10^{-2} eV/GPa	3.63	4.7	3.3
β	10^{-4}eV/GPa^2	−1.8	−18	−5.5

For the $Al_xGa_{1-x}N$/GaN violet LED, x *is* the Al fraction, when x=0.056, α and β can be calculated as 4.64×10^{-2} eV/GPa and -17.09×10^{-4} eV/GPa^2 according to Eq. (3) and Eq. (4), respectively. Similarly, for the $In_xGa_{1-x}N$/GaN-based blue light LED, when x=0.1, α and β can be obtained as 4.56×10^{-2} eV/GPa and -16.75×10^{-4} eV/GPa^2 according to Eq. (5) and Eq. (6), respectively.

$$\alpha(Al_xGa_{1-x}N) = x\cdot\alpha(AlN) + (1-x)\cdot\alpha(GaN) \tag{3}$$

$$\beta(Al_xGa_{1-x}N) = x\cdot\beta(AlN) + (1-x)\cdot\beta(GaN) \tag{4}$$

$$\alpha(In_xGa_{1-x}N) = x\cdot\alpha(InN) + (1-x)\cdot\alpha(GaN) \tag{5}$$

$$\beta(In_xGa_{1-x}N) = x\cdot\beta(InN) + (1-x)\cdot\beta(GaN) \tag{6}$$

The physical properties of most of semiconductor materials are sensitive to the stress, including the bandgap and peak wavelength, and undergo a red or blue shift [21,22]. Fig. 6 shows the relationships between the bandgap and the investigated stress levels of the violet and blue LED. The bandgap of the violet LED increases from 3.53 eV to 3.62 eV as the stress level rises from 0 GPa to 2 GPa, exhibiting a nearly linear trend. In the same stress range, the

blue LED displays a similar stress response to that of the violet LED, with the bandgap increasing from 2.95 eV to 3.04 eV. As can be seen in Fig. 6, an increase in stress results in a widening of the bandgap for both blue and violet LEDs, accompanied by a blue shift in the peak wavelength.

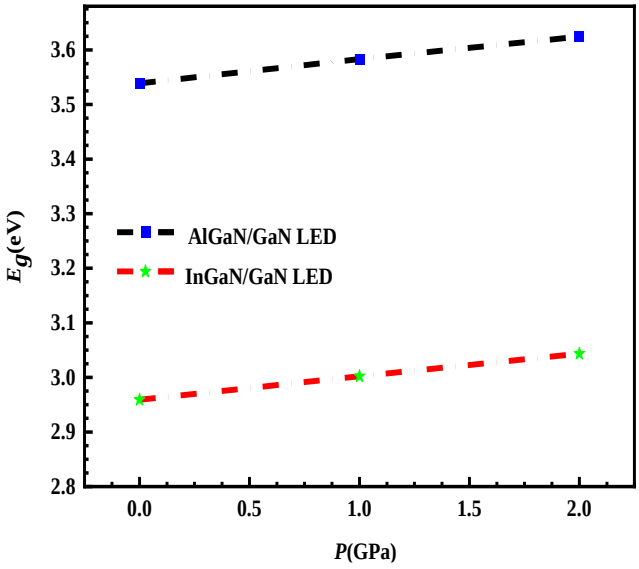

Fig. 6. The relationships between the bandgaps of violet LED and blue LED and the studied stress (color online)

3.5. Electrical properties

Fig.7 shows the relationships between the I-V characteristic curves and the investigated stress levels of the violet LED and blue LED, respectively. The extracted threshold voltages are shown in Tab. 2. As shown in Tab. 2, the threshold voltage of the violet LED exhibits an increase from 3.14 V to 3.31 V with the application of stress, whereas the threshold voltage of the blue LED demonstrates a rise from 2.81 V to 2.90 V under the same stress conditions. This suggests that both the violet and blue LEDs display an upward shift in their threshold voltage in response to the applied stress. Furthermore, the impact of stress on the threshold voltage of the violet LED is more pronounced than that observed in the blue LED.

Table 2. Threshold voltages of blue/violet LEDs under different stresses

LED type	Unit	0 GPa	1 GPa	2 GPa
Violet	V	3.14	3.26	3.31
Blue	V	2.81	2.86	2.90

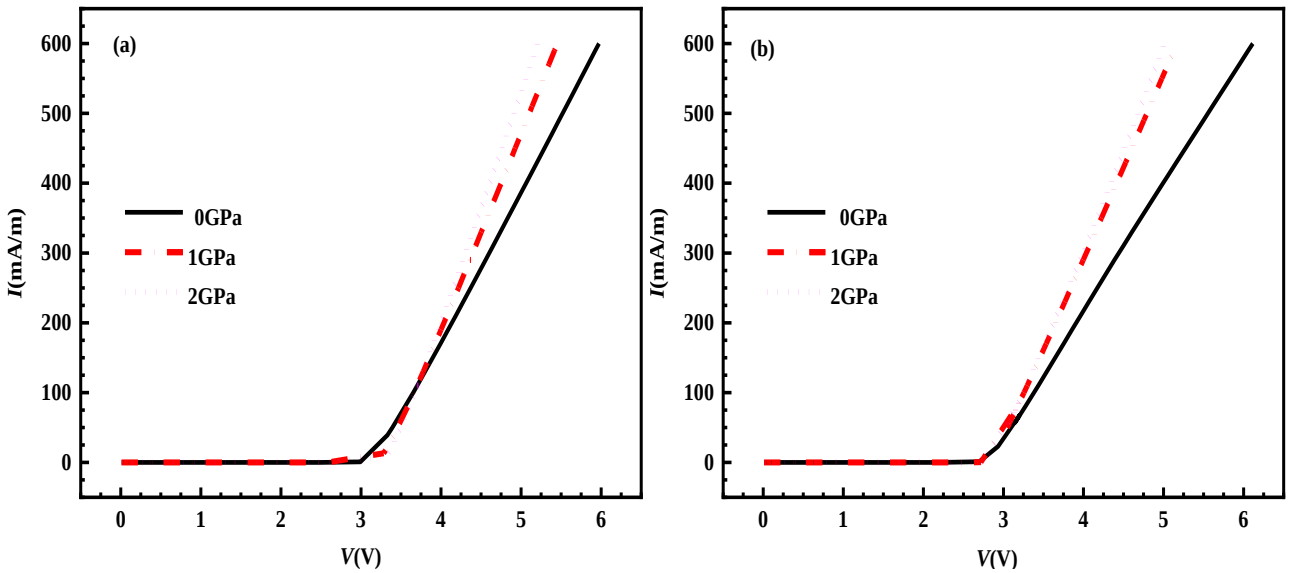

Fig. 7. I-V characteristic curves of LEDs under different stresses: (a) Violet LED; (b) Blue LED (color online)

4. Conclusion

This study investigates the stress-induced effect of the luminous and electrical properties of the AlGaN/GaN violet MQW LED and the InGaN/GaN blue MQW LED using APSYS software. The bandgap, carrier concentration, optical output power and threshold voltage demonstrated a pronounced stress-dependence under the studied conditions (0 GPa~2.0 GPa) in both the violet and blue LEDs. However, the stress-induced effect on the violet LED was observed to be more pronounced than that of the blue LED. The aforementioned conclusions provide a foundation for further research on the optimization and enhancement of the luminous and electrical properties of short-wavelength LEDs through the utilization of stress modulation.

Acknowledgments

This work is supported by Graduate Education Comprehensive Reform Research and Practice Project of Xi'an Shiyou University (NO.2023-X-YJG-024), 2023 Innovation and Entrepreneurship Training Program Project of Xi'an Shiyou University (NO.202310705016), and Xi'an Shiyou University Funding (NO. HX290023067)

References

[1] L. Shang, B. S. Xu, S. F. Ma, H. C. Ouyang, H. S. Shan, X. D.Hao, B. Han, Materials Science in Semiconductor Processing **146**, 146 (2022).
[2] Hongxia Li, Yuxin Lu, Tao Zhu, Rongxin Cao, Yuxiong Xue, Xianghua Zeng, Microelectronics Reliability **142**, 114915 (2023).
[3] Pengcheng Zhang, Qiuling Wen, Xipeng Xu, Optics Communications **464**, 125548 (2020).
[4] Dengkui Wang, Xian Gao, Jilong Tang, Xuan Fang, Dan Fang, Xinwei Wang, Fengyuan Lin, Xiaohua Wang, Rui Chen, Zhipeng Wei, Scientific Reports **11**(1), 676 (2021).
[5] Saroosh Rabia, Tauqeer Tauseef, Afzal Sara, Mehmood Haris, IET Optoelectronics **11**(4), 156 (2017).
[6] H. Yu, Q. Chen, Z. Ren, M. Tian, S. Long, J. Dai, C. Chen, H. Sun, IEEE Photonics **11**(4), 1 (2019).
[7] Minggang Liu, Yibin Yang, Peng Xiang, Weijie Chen, Xiaobiao Han, Journal of Chinese Physics B, **24**(6), 34 (2015).
[8] Miaochan Tsai, Shenghorng Yen, Shuhsuan Chang, Yenkuang Kuo, Optics Communications **282**(8), 1589 (2009).
[9] Yongjun Nam, Uiho Choi, Kyeongjae Lee, Taehoon Jang, Donghyeop Jung, Okhyun Nam, Journal of Vacuum Science and Technology B **38**(2), 103 (2020).
[10] Yoshihiro Sugawara, Yukari Ishikawa, Arata Watanabe, Makoto Miyoshi, Takashi Egawa, Japanese Journal of Applied Physics **55**(5S), 45 (2016).
[11] Chong Xing, Huabin Yu, Zhongjie Ren, Haochen Zhang, Jiangnan Dai, Changqing Chen, Haiding Sun, IEEE Journal of Quantum Electronics **56**(1), 1(2020).
[12] Muhammad Usman, Abdur-Rehman Anwar, Kiran Saba, Munaza Munsif, Optik **215**, 164767 (2020)
[13] Yingying Lin, Hadi Sena, Martin Frentrup, Markus Pristovsek, Yoshio Honda, Hiroshi Amano, Journal of Applied Physics **133**(22), 225702 (2023).
[14] Danghui Wang, Tianhan Xu, Fang Chen, Journal of Optoelectronics and Advanced Materials **19**(7-8), 517 (2017).
[15] Longfei He, Kang Zhang, Hualong Wu, Chenguang He, Wei Zhao, Qiao Wang, Shuti Li, Zhitao Chen, Journal of Materials Chemistry C **9**(25), 7893 (2021).
[16] C. Chu, K. Tian, J. Che, H. Shao, J. Kou, Y. Zhang, Y. Li, M. Wang, Y. Zhu, Z. H. Zhang, Optics Express **27**(12), A620 (2019).
[17] Satyam S. Parashari, S. Kumar, S. Auluck, Solid-State Electronics **52**(5), 749 (2008).
[18] I. Gorczyca, N. E.Christensen, Physica B: Condensed Matter **185**(1–4), 410 (1993).
[19] P. Perlin, I. Gorczyca, N. E. Christensen, I. Grzegory, H. Teisseyre, T. Suski, Physics Review B **45**(23), 13307 (1992).
[20] Yifeng Duan, Lixia Qin, Liwei Shi, Gang Tang, Journal of Computational Materials Science **101**, 56 (2015).
[21] Ye Yu, Tao Wang, Xiufang Chen, Lidong Zhang, Yang Wang, Yunfei Niu, Jiaqi Yu, Haotian Ma, Xiaomeng Li, Fang Liu, Gaoqiang Deng, Zhifeng Shi, Baolin Zhang, Xinqiang Wang, Yuantao Zhang, Light: Science and Applications **10**(1), 117 (2021).
[22] Wenbin Lv, Lai Wang, Lei Wang, Yuchen Xing, Di Yang, Zhibiao Hao, Yi Luo, Applied Physics Express **7**(2), 343 (2014).

*Corresponding author: wdhyxp@outlook.com